

**Sarcoma Cell Line Screen of Oncology Drugs and Investigational Agents Identifies
Patterns Associated with Gene and microRNA Expression**

Beverly A. Teicher^{2,4}, Eric Polley³, Mark Kunkel², David Evans¹, Thomas Silvers¹, Rene Delosh¹, Julie Laudeman¹, Chad Ogle¹, Russell Reinhart¹, Michael Selby¹, John Connelly¹, Erik Harris¹, Anne Monks¹, Joel Morris²

¹Molecular Pharmacology Group, Leidos Biomedical Research, Inc., Frederick National Laboratory for Cancer Research, Frederick, Maryland, 21702; ²Developmental Therapeutics Program, Division of Cancer Treatment and Diagnosis, National Cancer Institute, Rockville, Maryland 20852; ³Biometric Research Branch, Division of Cancer Treatment and Diagnosis, National Cancer Institute, Rockville, Maryland 20852

Running Title: Sarcoma Cell Line Screen

Key Words: Sarcoma; sarcoma cell-based screen; sarcoma microRNAs, sarcoma gene expression

Financial Information: This project has been funded in whole or in part with federal funds from the National Cancer Institute, National Institutes of Health, under Contract No.

HHSN261200800001E. The content of this publication does not necessarily reflect the views or policies of the Department of Health and Human Services, nor does mention of trade names, commercial products, or organizations imply endorsement by the U.S. Government. This research was supported [in part] by the Developmental Therapeutics Program in the Division of Cancer Treatment and Diagnosis of the National Cancer Institute.

Conflict of interest: The authors declare that they have no conflicts of interests to report.

⁴Corresponding author: Beverly A. Teicher, PhD
Chief, Molecular Pharmacology Branch
National Cancer Institute
RM 4-W602, MSC 9735
9609 Medical Center Drive
Bethesda, MD 20892
Phone: 240-276-5972
FAX: 240-276-7895
Email: Beverly.Teicher@nih.gov
Email: teicherba@mail.nih.gov

ABSTRACT

The diversity in sarcoma phenotype and genotype make treatment of this family of diseases exceptionally challenging. Sixty-three human adult and pediatric sarcoma lines were screened with 100 FDA approved oncology agents and 345 investigational agents. The investigational agents library enabled comparison of several compounds targeting the same molecular entity allowing comparison of target specificity and heterogeneity of cell line response. Gene expression was derived from exon array data and microRNA expression was derived from direct digital detection assays. The compounds were screened against each cell line at 9 concentrations in triplicate with an exposure time of 96 hrs using Alamar blue as the endpoint. Results are presented for inhibitors of the following targets: aurora kinase, IGF-1R, MEK, BET bromodomain, and PARP1. Chemical structures, IC₅₀ heat maps, concentration response curves, gene expression and miR expression heat maps are presented for selected examples. In addition, two cases of exceptional responders are presented. The drug and compound response, gene expression and microRNA expression data are publicly available at <http://sarcoma.cancer.gov>. These data provide a unique resource to the cancer research community.

INTRODUCTION

Sarcomas are cancers of mesodermal origin that arise from connective tissue (soft-tissue sarcoma) or bone (osteosarcoma, chondrosarcoma) (1). Sarcomas are rare tumors, about 1% of all human cancers. Many of these tumors affect children and young adults accounting for 15% of all pediatric cancers. There are approximately 13,000 cases of sarcoma diagnosed per year in the USA and an estimated death rate around 4,500 patients. Soft tissue sarcoma (STS) is a diverse group of tumors comprising over 50 subtypes, the most common of which are liposarcoma, derived from adipose tissue and leiomyosarcoma, derived from smooth muscle. Certain sarcoma types are primarily pediatric, e.g., osteosarcoma, Ewing's sarcoma/primitive neuroectodermal tumors (PNET, sometimes classified with the bone sarcomas) and rhabdomyosarcoma, while others are most common in adults over 55 years of age, e.g., leiomyosarcoma, synovial sarcoma and liposarcoma (2,3).

Sarcomas are classified by the abnormalities that drive their pathogenesis. However, most sarcoma subtypes are still treated with traditional therapeutic modalities. Surgery with or without adjuvant or neoadjuvant radiation is the most common treatment for localized disease. Over half of sarcoma patients develop metastatic disease which is treated with chemotherapy. Doxorubicin and ifosfamide are the two most active agents in advanced soft tissue sarcoma with an average response rate of 20% (4). Several core molecular determinants of sarcomagenesis have been identified and have the potential to transform the care of sarcoma patients (5). Chromosomal translocations occur in about one-third of sarcomas (6). The majority of sarcomas have nonspecific genetic changes with a complex karyotype (7).

The challenge in sarcoma research for diseases such as chondrosarcoma is finding therapeutically tractable targets. Approximately 30% of mesenchymal tumors carry a specific translocation with an otherwise relatively simple karyotype. The fusion proteins act either as transcription factors, up-regulating genes responsible for tumor growth, as for Ewing's sarcoma, or translocate a highly active promoter in front of an oncogene driving tumor formation, as for aneurysmal bone cyst (8). Molecular studies have identified oncogenic pathways in sarcomas which can be targeted by drugs that include histone deacetylases in translocation associated sarcomas of young adults, Akt/mammalian target of rapamycin (mTOR) inhibitors in pleomorphic sarcomas, and macrophage colony-stimulating factor in giant cell tumor of bone (9). While in many cancers, the age of the patient influences treatment; this is less often the case with sarcoma (10).

The rare incidence of each sarcoma subtype makes clinical trials challenging. Trials often enroll patients with any sarcoma subtype, despite diverse epidemiologies, pathogenesises, etiologies and clinical manifestations, resulting in highly heterogeneous patient cohorts (4, 11). The promise of molecular personalized medicine is being realized in sarcoma with the success of imatinib mesylate and sunitinib in gastrointestinal stromal tumors (GIST) (12, 13). In addition, imatinib has shown activity in metastatic dermatofibrosarcoma protuberans (DFSP) and fibrosarcomatous DFSP (14). Ceritinib, a targeted ALK inhibitor, has shown activity in pediatric inflammatory myofibroblastic tumor and shows promise in clear cell sarcoma (15). At the recommended Phase II dose, mTOR inhibitor sirolimus along with the HDAC inhibitor vorinostat demonstrated activity in perivascular epithelioid cell tumor (PEComa) (16). Cediranib, a potent inhibitor of all three VEGFRs, has demonstrated an overall response rate of 35% and a disease control rate of 84% at 24 weeks in alveolar soft part sarcoma (17). Another

antiangiogenic kinase inhibitor, pazopanib, has been approved for treatment of metastatic soft tissue sarcoma (**18, 19**).

The current study was undertaken to explore the response of a wide spectrum of sarcoma cells lines to approved anticancer drugs and to a library of investigational agents in conjunction with exon arrays and microRNA array results to allow correlation of molecular characteristics with compound response. These data are publicly available at: <http://sarcoma.cancer.gov>.

MATERIALS AND METHODS

Cell Lines. Division of Cancer Treatment and Diagnostics of the National Cancer Institute (DCTD/NCI) collected a panel of 63 human adult and pediatric sarcoma cell lines. Cells were purchased from ATCC (Manassas VA), or obtained from Dr. Samuel Singer (Memorial Sloan Kettering Cancer Center, NY, NY), the Children's Oncology Group (COG; Dr. Patrick Reynolds, Texas Tech University Health Sciences Center, Lubbock, TX) and Dr. Peter Houghton (Nationwide Children's Hospital, OHSU). The atypical synovial sarcoma cell line, SW982 expresses SSX gene, but not SYT-SSX or HLA-A24 (**Supplemental Figure 1**). The ASPS-1 aveolar soft part sarcoma line was developed at NCI (**20**). The sarcoma lines were stored frozen at 10^6 cells per ml in liquid nitrogen. The sarcoma lines were authenticated using the Applied Biosystems Identifiler kit for short tandem repeat analysis (15 loci). The lines were thawed from the banked stock and samples were taken for Identifiler analysis within passages 2-5. New cells from the same frozen stock were thawed after a maximum of 20 passages, which did not exceed 5 continual months in culture. The human A549 NSCLC line purchased from ATCC was run on each plate as a screen control. The lines were maintained in the medium specified for each line supplemented with fetal bovine serum and other additives (**Supplemental Table 1**).

Compounds. Approximately 100 FDA-approved anticancer drugs (available from NCI at: http://dtp.nci.nih.gov/branches/dscb/oncology_drugset_explanation.html) and a library of 345 investigational oncology agents, composed primarily of targeted small molecules currently in

clinical and/or preclinical studies acquired by synthesis or purchase were screened against the 63 sarcoma cell line panel (**Supplemental Table 2**).

Screen. Twelve lines (11 sarcoma and A549 human NSCLC cell line control) were screened per run. Each of the 12 lines was grown and harvested using standard tissue culture procedures. On day 1, the cells were collected and suspended at the desired density in 300 ml of media. The cells were plated using a Tecan Freedom Evo robotic device. A cell inoculum (42 ul) was added to designated wells in 384-well plates (15 test plates, 1 Control plate). After cell inoculation, the plates were moved to a humidified 37°C incubator with 5% CO₂. The next day, the Tecan Evo was used to perform compound addition. Each compound was tested at 9 concentrations ranging from 10 uM to 1.5 nM (final DMSO concentration 0.25%). After compound addition, the plates were returned to the humidified 37°C incubator for 96 hrs incubation. The controls were: topotecan (10uM); doxorubicin (10uM); tamoxifen (200uM); and DMSO (0.25%). The incubation was terminated by adding Alamar blue solution (15 ul) to each well using the Tecan Evo, the plates were incubated 4hr in a humidified 37°C incubator and fluorescent signal in the wells were read on a Tecan plate reader.

Exon and MicroRNA Arrays. Total RNA including the miRNA fraction was extracted from samples using Qiagen miRNeasy Mini Kit (Qiagen, Valencia CA) according to manufacturer's instructions. Agilent RNA Integrity Number (RIN) >8.5 indicated good quality RNA for all samples. Sense strand cDNA from 100ng total RNA was fragmented and labeled using Affymetrix WT terminal labeling kit. Samples were hybridized with Human Exon 1.0 ST Arrays (Affymetrix) at 45⁰C, 60 rpm for 16 hrs. Arrays were washed and stained using Affymetrix Fluidics Station 450 and scanned on Affymetrix GeneChip scanner 3000 7G.

Expression data from mRNA was normalized using Robust Multi-Array Average (RMA) and summarized at the gene level using AROMA (21). Exon array data is available at GSE68591.

For microRNA profiling, total RNA (100 ng) was ligated to unique oligonucleotide tags to increase the length of the short miRNA for detection without amplification using the NanoString kit. Samples were hybridized for 16 hrs to NanoString human miRNA probeset which has probe pairs specific for each miRNA with different fluorescent barcode labels. Each consists of a Reporter Probe, with the fluorescent signal on its 5' end, and a Capture Probe with biotin on the 3' end. Purification of bound probes was performed with a two-step magnetic bead-based wash on the nCounter™ Prep Station followed by immobilization in the cartridge for data collection. The miRNA data was scale normalized and log₂ plus 1 transformed. The miRNA expression data is available at GSE69470.

Data Analysis. Concentration response data were fit with a 4 parameter curve fit and IC₅₀s determined. The data are publicly available at: <http://sarcoma.cancer.gov>. Hierarchical clustering of gene expression was performed for drugs with greatest IC₅₀ variability across the cell lines. Average linkage clustering using 1 - Pearson correlation distance was performed. Pair-wise Pearson correlations between the negative log₁₀ IC₅₀ and log₂ gene or miRNA expression are presented. The Affymetrix mRNA and the NanoString microRNA data sets supporting the results of this article are available for direct download from the Gene Expression Omnibus (<http://www.ncbi.nlm.nih.gov/geo/>). The accession number for the overall project is GSE69524 (<http://www.ncbi.nlm.nih.gov/geo/query/acc.cgi?acc=GSE69524>), Affymetrix: GSE68591 (<http://www.ncbi.nlm.nih.gov/geo/query/acc.cgi?acc=GSE68591>), and Nanostring: GSE69470 (<http://www.ncbi.nlm.nih.gov/geo/query/acc.cgi?acc=GSE69470>).

RESULTS

The sarcoma lines performed well in the screen with an average Z' value of 0.85 and an average signal to background of 15.8. Topotecan, doxorubicin and tamoxifen were included in each run to assess screen stability (**Supplemental Figure 2**). When the data were analyzed by unsupervised clustering of compounds and cell lines, clear patterns emerged (**Supplemental Figure 3**).

To analyze the relationships between the compounds tested, any agents with a $\log_{10} IC_{50}$ range < 0.5 across the 63 cell lines were removed, as these agents will have low statistical power to detect pair-wise associations. After the filtering, 345 compounds (out of 445 tested) remained. A constellation relational map for the approved and investigational agents tested in the sarcoma lines was developed. The drugs and compounds were connected with a line if the pair-wise correlation of the $\log_{10} IC_{50}$ was greater than 0.75 with thickness of the line indicating greater correlation (**Figure 1**). The relational map identified clusters of compounds which had highly correlated patterns of cell line sensitivity. Many of the compound clusters could be classified based on the same molecular target or pathway and others based on similar cellular effects such as DNA damage. Some of the clusters such as the MEK cluster included compounds developed to target the same protein while other clusters included compounds developed to target varied proteins.

The investigational agents tested included 8 aurora kinase inhibitors (**Figure 2A**). The heat map (generated using the website) for the aurora kinase inhibitors across 63 sarcoma lines showed the great heterogeneity in cell line response (as measured by 50% inhibitory

concentration, IC_{50}) to the aurora kinase inhibitors with the Ewing sarcoma and the synovial sarcoma lines being more sensitive as a group to these compounds than the other sarcoma line panels (**Figure 2B**). The differential response of the sarcoma lines to the aurora kinase inhibitors spanned the entire concentration range tested from 10 μ M to 1 nanomolar. For the heat maps and IC_{50} estimates, cell lines for which an IC_{50} was not reached are included as the lowest or highest concentration tested. The mean IC_{50} s for these compounds was from 0.23 μ M to < 0.013 μ M. The most clinically advanced aurora kinase inhibitor, alisertib (NSC759677), is currently in Phase III clinical trial. The mean IC_{50} for alisertib in the sarcoma lines was 0.135 μ M and the mean IC_{50} in the Ewing lines was 0.028 μ M. The clinical C_{max} concentration of alisertib is 2-6 μ M, thus, the screen results suggest that Ewing sarcoma and synovial sarcoma may be susceptible to alisertib at clinically achievable concentrations. Barasertib (NSC 757444) is in Phase II clinical trial and has an active metabolite clinical steady state concentration of 0.45 μ M. The mean IC_{50} for barasertib in the sarcoma lines was 0.23 μ M and the mean IC_{50} in the Ewing sarcoma lines was 0.019 μ M. However, even among the Ewing lines there appears to be a range of sensitivities upon exposure to this compound with the less sensitive lines comprising 4 out of 19 of the panel (**Figure 2C**).

The IGF-1R kinase inhibitors presented a more complex pattern (**Figures 3A and B**). There was a consistent sub-group of rhabdomyosarcoma lines (Rh-30, SJCRH30, Rh-28, Rh-28 PX11/LPAM and Rh-41) that were more sensitive to the IGF-1R kinase inhibitors (**Figure 3C**). All of these lines are alveolar rhabdomyosarcoma-with relatively high expression of ALK, anaplastic lymphoma tyrosine kinase. The embryonal rhabdomyosarcoma lines (Hs 729, RD and Rh36) are less sensitive to IGF1R inhibitors and are lower expressers of ALK kinase. Sensitivity to the IGF-1R inhibitor linsitinib (NSC756652) compared with gene expression data for ALK (r

= 0.54), IGF-2 ($r = 0.03$), IGF-1 ($r = 0.51$) and IGF-1R ($r = 0.11$) and microRNAs miR-9 ($r = 0.59$), miR-100 ($r = -0.58$), miR-222 ($r = -0.57$), miR-125 ($r = -0.52$), miR-22 ($r = -0.52$) and miR-21 ($r = -0.61$). This indicates that high levels of miR-9 and low levels of the other miRs correlated better with sensitivity to linsitinib than high gene expression for the putative protein targets (**Figure 3D**). The expression of miR-9-5p was higher in Ewing sarcoma, synovial sarcoma and subsets of rhabdomyosarcoma and osteosarcoma lines than in normal cells and other sarcoma lines (**Supplemental Figure 4**). All of the miRs that were negatively correlated with response to linsitinib were expressed at higher levels in normal cells, chondrosarcoma, liposarcoma, leiomyosarcoma and malignant peripheral neural sheath tumor lines than in other sarcoma lines.

The sarcoma lines were, generally, insensitive to the MEK inhibitors; however, a subset of lines was sensitive to certain MEK inhibitors (**Figures 4A and B**). Among the MEK inhibitors, trametinib (NSC758246) in combination with dabrafenib (BRAF inhibitor) is approved for treatment of mutant B-Raf melanoma, selumetinib (NSC764042) is in Phase III trial (NCT01933932, NCT01843062, NCT01974752) and refametinib (NSC765866) is in Phase II trial (NCT02168777, NCT01915589, NCT01915602). Four sarcoma lines, HT-1080 fibrosarcoma which expresses mutant NRASp.Q61K, ES-4 Ewing sarcoma, RD rhabdomyosarcoma and Rh36 rhabdomyosarcoma which all express mutant NRAS(p.Q61K), are sensitive to trametinib, however, the concentration response curves lack sigmoid shape. The mean IC_{50} across the four (lines of 0.016 μM is less than the clinical C_{max} of 0.036 μM for the drug (**Figure 4C**). In those same lines selumetinib had a mean IC_{50} of 5 μM , which is slightly above the clinical C_{max} of 3.2 μM for the compound. The mean IC_{50} for the eight MEK inhibitors across the sarcoma lines was 3.55 μM with a range of 0.032 μM to 10 μM (**Figures 4B and C**).

The PI3K/Akt/mTOR pathway was an effective drug target in a subset of sarcoma lines (**Supplemental Figure 5**). Sarcoma lines sensitive to compounds targeting the PI3K/Akt/mTOR pathway included SK-UT-1B leiomyosarcoma, Rh41 and Rh28 PX11/LPAM rhabdomyosarcoma and CHLA-10 Ewing sarcoma. The KHOSNP, KHOS-240S and KHOS-312H osteosarcoma lines were resistant to compounds targeting each of these three kinases.

The BET bromodomain inhibitors JQ1 (NSC764043) and I-BET-151 (NSC767599) are shown in **Figure 5A**. By gene expression, MYC (cMyc) was, generally, highest in Ewing sarcoma and synovial sarcoma, MYCN (nMyc) expression was highest in the rhabdomyosarcoma lines, and RUNX2, another potential bromodomain binding transcription factor, was most highly expressed by the osteosarcoma lines and the bone/muscle lines. The liposarcoma line LS141 has high expression of both MYC and RUNX2 (**Figure 5C**). The mean IC_{50} for the BET bromodomain inhibitors JQ1 and I-BET-151 across the sarcoma lines was low micromolar; however, the primary targets of the compounds may be different in the sarcoma subgroups. The mean IC_{50} for JQ1 across the sarcoma lines was 0.83 μ M with a range of 0.065 to 10 μ M (**Figure 5B**). Synovial sarcoma was the most sensitive subgroup with a mean IC_{50} of 0.25 μ M and a range of 0.065 -0.59 μ M and the line SYO-1 was the most sensitive sarcoma line with an IC_{50} of 0.065 μ M. For osteosarcoma the mean IC_{50} was 0.8 μ M and the range was 0.093 to 7.41 μ M with the OHS line being most sensitive (IC_{50} 0.93 μ M) and for rhabdomyosarcoma the mean IC_{50} was 2.29 μ M with a range of 0.16 μ M to 10 μ M with Rh41 being the most sensitive (IC_{50} 0.158 μ M) (**Figure 5D**). The Pearson correlation coefficient for expression of cMYC and sensitivity to JQ1 was 0.35 indicating that high expression of MYC mRNA was positively associated with sensitivity to JQ1.

The chemical structure for the potent PARP inhibitor talazoparib (BMN673, NSC767125) is shown in **Figure 6A**. The expression of genes related to response to DNA damage, BRCA1, BRCA2, PARP1, PARP2, and RAD51, in the sarcoma lines are shown in **Figure 6B**. Five sarcoma lines including the chondrosarcoma SW1353, the two malignant peripheral neural sheath tumor lines MPNST and ST8814, the rhabdomyosarcoma Rh36 and the atypical synovial sarcoma SW982 have relatively low expression of all 5 genes. Five PARP1 inhibitors were tested in the sarcoma lines (**Figure 6B**). The mean IC₅₀ for talazoparib across the sarcoma lines was 0.29 uM with a range of 0.0015 to 10 uM (**Figure 6C**). The mean IC₅₀ for the Ewing sarcoma lines to talazoparib was 0.051 uM with a range of < 0.0015 to 0.83 uM. The malignant peripheral neural sheath tumors, which by gene expression had very low levels of PARP1 had a mean IC₅₀ to talazoparib of 0.24 uM, very near the mean of all of the lines, with a range of 0.067 to 0.85uM. The mean IC₅₀ of talazoparib for the synovial sarcoma lines was 0.049 uM with a range of <0.0018 uM to 0.41 uM. The SYO1 synovial sarcoma line was greater than 1 log more sensitive to talazoparib than were the other two synovial sarcoma lines. The **Figure 6D** heat map shows a trend that higher expression of PARP1 ($r = 0.54$), and to a lesser extent, BRCA1 ($r = 0.14$) and BRCA2 ($r = 0.16$) correlated with greater sensitivity to talazoparib while expression of PLK2 was negatively correlated with sensitivity to talazoparib ($r = -0.76$). The exceptional lines, MPNST, ST8814, SW982, Rh36 and SW1353, with very low gene expression can be seen on the heat map. High levels of the microRNAs, miR-150 ($r = 0.55$) and miR-9 ($r = 0.64$) correlate positively with sensitivity to talazoparib while low levels of microRNAs miR-574 ($r = -0.58$), miR-22 ($r = -0.71$), miR-21 ($r = -0.62$), miR-30 ($r = -0.59$) and miR-100 ($r = -0.55$) correlate negatively with sensitivity to talazoparib. Four of the miRs which correlate with response to talazoparib are the same as those that correlate with response to linsitinib. Of the

remaining, miR-150 which correlated positively with sensitivity to talazoparib has low expression in normal cells and most sarcoma lines and was higher in Ewing sarcoma (**Supplemental Figure 6**). MiR-574 was expressed at higher levels in normal cells than in most sarcoma lines and miR-30 has a mixed pattern.

Exceptional responders can provide important leads for molecular targets. There were examples of exceptionally responsive sarcoma lines. The A-204 rhabdoid tumor line was exceptionally responsive to the IAP inhibitor birinapant (NSC767128) with an IC_{50} of 0.058 μ M compared with >10 μ M for all other sarcoma lines except HSSY-II which had an IC_{50} of 2 μ M. (**Supplemental Figures 7 and 8**). MiR-204 expression was highly positively correlated with the A-204 birinapant response ($r = 0.82$). The A-673 Ewing sarcoma line was exceptionally responsive to three kinase inhibitors, saracatinib (NSC758872), ZM-336372 (NSC756654) and WZ-4002 (NSC755927). With each of these compounds the sensitivity of the A-673 line reached an IC_{50} of < 0.0015 μ M, the lower limit of the screen. The expression of FRG2, which codes for a protein normally expressed only in myoblasts and whose overexpression has been associated with facioscapulohumeral muscular dystrophy, was highly correlated with the response of the A-673 cells to the three kinase inhibitors ($r = 0.68, 0.78, \text{ and } 0.77$, respectively) (**Supplemental Figure 9**) (22).

DISCUSSION

The great diversity in sarcoma phenotypes and genotypes make this disease family exceptionally challenging. Phenotypically diverse human adult and pediatric sarcoma lines were screened with a defined set of drugs and compounds (23). Sarcoma genomics have been explored using cell lines and clinical specimens (13, 24). The current study presents gene expression data derived from exon array data as well as microRNA data, which are available in GEO.

One study goal was to identify small molecule drugs for further examination in sarcoma. The constellation relational map provides visualization of the sarcoma screen for compounds with a dynamic range of at least one log in IC_{50} across the panel (Figure 1). The clusters are compounds with similar patterns of cell line response. Aurora kinase inhibitors form a distinct cluster adjacent to bifunctional alkylating agents, topoisomerase I and II inhibitors. Taxanes and microtubule fragmenters form a cluster adjacent to topoisomerase I and II inhibitors. The results are consistent with DNA damage being an important factor in the cytotoxicity of these agents. Other classes of agents such as proteasome inhibitors, dihydrofolate reductase inhibitors and HSP90 inhibitors form clusters that are not connected, supporting the notion that these compounds have unique mechanisms. Some clusters include compounds with more than one putative target, e.g., mTOR and Akt inhibitors cluster together. The results underscore the ability of a cell line panel response pattern to elucidate putative molecular targets and cell similarities.

Aurora kinases are nuclear serine/threonine kinases essential for cell division (25). The potency of aurora kinase inhibitors led to their classification as cytotoxic agents (26). The response of the sarcoma lines to aurora kinase inhibitors was heterogeneous, with clear selectivity for Ewing sarcoma and synovial sarcoma lines (Figure 2). Aurora kinase inhibitors are in clinical trials in hematologic malignancies and solid tumors (27) and are in Phase II

clinical trials in a broad spectrum of adult soft tissue sarcoma. Preclinically, pediatric sarcoma are sensitive to aurora kinase inhibitors; however, clinical trials have not yet been initiated (28). In pediatric sarcoma xenograft studies, alisertib (NSC759677) had activity in rhabdomyosarcoma xenografts but little activity against Ewing sarcoma xenografts (29); however, higher doses higher than can be achieved in humans were used (30).

The insulin-like growth factors and the insulin-like growth-1 receptor (IGF-1R) are targeted by multiple small molecules and multiple antibody therapeutics . A predictive biomarker for IGF/IGF-1R targeted agents is being sought (31). The current screen data highlighted some of the challenges (Figure 3). While subgroups of several sarcoma types respond to the IGF-1R inhibitors, others do not. There was a positive correlation between response to the IGF-1R inhibitor linsitinib and ALK gene expression ($r = 0.54$) and weak correlation with IGF-1R ($r = 0.11$). MiR-9-5p expression was positively correlated ($r = 0.59$) with sensitivity to linsitinib while the expression of miRs 100-5p, 222-3p, 125b-5p, 22-3p and 21-5p were negatively correlated. MiR-9 and miR-21 are associated with insulin resistance and diabetes-associated pancreatic cancer, and thus, with the insulin/IGF signaling pathway (32). Although miR-9 is an oncogenic miR, linked with high c-Myc expression (33), it is also associated with BRCA1 down-regulation and decreased DNA damage repair, thus, improving response to chemotherapy (34). MiR-21, another oncogenic miR (35), downregulated expression of the tumor suppressor IGFBP3 (36). Data indicate that miR-100 acts as a tumor suppressor in chondrosarcoma and overexpression in chondrosarcoma and can increase sensitivity to chemotherapy (37). MiR-100 appears to target the FKBP51 and IGF1R/mTOR signaling pathways (38). These data indicate that microRNAs may be important in determining response to IGF-1R inhibitors.

The RAS/RAF/MEK/ERK and the PI3K/AKT/mTOR pathways are frequently altered in cancer (39). The single agent MEK inhibitor activity across the sarcoma lines was modest; however, specific lines from varied sarcoma types were sensitive to MEK inhibition (Figure 4 A-C). Among the sensitive lines, the HT-1080 fibrosarcoma and the rhabdomyosarcoma lines RD and Rh36 express mutant RAS (40). However, the MEK inhibitor, selumetinib (NSC764042) was not effective against the Rh36 xenograft (31). Hu09 osteosarcoma was sensitive to inhibitors of RAS/RAF/MEK/ERK while the KHOS lines were not (Figure 4D). Finally, the Rh41, Rh28 PX11/LPAM and SJCRH30(RMS13) rhabdomyosarcoma lines were sensitive to inhibitors of the PI3K/AKT/mTOR pathway while the Rh36 and Rh28 lines were not (41). Both Akt inhibitors and mTOR inhibitors had little activity against rhabdomyosarcoma and Ewing sarcoma xenografts (42-45). The MEK inhibitor PD-0325901 is in clinical trial for adolescent and adults with neurofibromatosis type-1 (NF1), a genetic disease with a predisposition for patients to rhabdomyosarcoma. The MEK inhibitors, trametinib and MEK162 are undergoing broad spectrum clinical trials (ClinicalTrials.gov Identifiers NCT02096471, NCT01991379, NCT01725100 and others).

The bromodomain and extraterminal (BET) protein, Brd4, described as a general transcriptional regulator (e.g., Myc), recruits transcriptional regulatory complexes to acetylated chromatin (46). The therapeutic effects of bromodomain inhibitors have been attributed to a specific set of downstream target genes whose expression are sensitive to BET protein targeting. JQ1 and I-BET-151 have high affinity for bromodomains of the BET family (47). Among sarcoma, rhabdomyosarcoma express MYCN; in addition, Myc is positively regulated by EWS-FLI1 in Ewing sarcoma likely through an indirect mechanism (48). MYC transcript can be down-regulated by siRNA against EWS-FLI1 (49). MYC was expressed broadly by the sarcoma

lines with exceptions being ASPS-1 and osteosarcoma, and lower expression by fibrosarcoma and rhabdomyosarcoma (**Figure 5**). MYCN was expressed by a subset of rhabdomyosarcoma lines. Bromodomain inhibitors are in Phase 1 clinical trial in hematological malignancies, NUT (nuclear protein in testis) midline carcinoma, lymphoma and advanced solid tumors (ClinicalTrials.gov Identifiers NCT01713582, NCT01587703, NCT01949883, and NCT01987362).

PARP1, a highly expressed DNA binding protein, is involved in chromatin modification, transcription and DNA repair (**50**). Ewing sarcoma express high PARP1 and are sensitive to PARP1 inhibitors (**51, 52**). The EWS-FLI1 and EWS-ERG fusion proteins expressed in Ewing sarcoma induce DNA damage which is increased in the presence of PARP1 inhibition (**53**). However, a small clinical study of olaparib in refractory Ewing sarcoma resulted in no significant responses or durable disease control (**54**). Talazoparib as a single agent was not active against Ewing sarcoma xenografts (**55**). Rhabdomyosarcoma also tend to high in PARP1 (**Figure 6**) (**56**). Expression of polo-like kinase 2 (PLK2) and miRs -100, -574, -22, -21 and -30 were negatively correlated with talazoparib sensitivity (**Figure 6**). MiR-22 is repressed in Ewing sarcoma expressing EWS-FLI1, and was low in leiomyosarcoma and miR-22 expression was negatively correlated with sensitivity to talazoparib (**57**). In addition, cMyc expression can produce a down regulation of miR-22 (**58**). MiR-30, a tumor suppressor, is frequently down regulated in malignant disease (**59**). MiR-150 is upregulated in serum exosomes in colon cancer patients and downregulated in pancreatic cancer patients (**60**). In the sarcoma panel, high miR-150 was associated with sensitivity to talazoparib (**Figure 6**). Talazoparib is in active clinical trials including Phase 2 trials (ClinicalTrials.gov Identifiers NCT02116777, NCT02049593, NCT01286987, NCT01989546, NCT02127151, NCT01945775 and NCT02034916).

Inhibitors of apoptosis protein (IAP) are involved in regulating the caspase activation of NF- κ B signaling (61). Birinapant is a small molecule that mimics the binding of the endogenous IAP antagonist Smac to IAP proteins (62). The A-204 rhabdoid tumor line was an exceptional responder to the IAP inhibitor birinapant (Supplemental Figures 7 and 8). High miR-204 correlated with the sensitivity of the A-204 line to birinapant. High miR-204 is associated with slower tumor growth in malignant peripheral nerve sheath tumors and cholangiocarcinoma (63). On the other hand, miR-204 upregulation increased cell motility and migration in mesenchymal neural crest cells during development (64).

The A-673 Ewing sarcoma was an exceptional responder to three kinase inhibitors: saracatinib, an inhibitor of the non-receptor protein tyrosine kinase c-Src (65), WZ-4002, an EGFR T790M-mutant selective kinase inhibitor (66), and ZM-336372, a Raf inhibitor which blocks the Raf/MEK/ERK signaling pathway (67) (Supplemental Figure 9). A-673 cells have high phosphorylated Src protein and are sensitive to Src inhibition (68). High expression of FRG2 mRNA correlated with A-673 cell exceptional kinase inhibitor sensitivity. FRG2 is implicated in the genetic disease facioscapulothoracic muscular dystrophy (FSHD) and under normal condition in myogenesis (22, 69).

Many sarcoma lines screened in the current study have been in culture for > 20 years. Over time, the cultures may have genetically drifted from the original tumor, so that interpretation of the data based solely on histology of the tumor of origin may not be sufficient. Developing new xenografts and cell lines is especially important in sarcoma where many rare diseases are underrepresented or not represented by cell lines. In the sarcoma cell line panel, the bone sarcomas are well represented (both Ewing sarcoma and osteosarcoma); however, other sarcomas are absent or underrepresented, such as uterine LMS, myxoid liposarcomas,

dedifferentiated liposarcoma, undifferentiated pleomorphic sarcomas, and other rare subtypes. The current findings illustrate the complexity of correlating drug sensitivity in cell lines with nucleic acid measurements. A next step is to test promising findings from this screen in sarcoma xenograft models. The sarcoma website presents a facile venue to identify sarcoma cell line sensitivity to multiple approved and investigational agents. The cell line response can be associated with gene and miRNA expression and potentially lead to identification of disease targets or predictive biomarkers. All of the sarcoma screen data including the gene and miRNA expression data are publically available at <http://sarcoma.cancer.gov>.

REFERENCES

1. Kotilingam D, Lev DC, Lazar AJ, Pollock RE. Staging soft tissue sarcoma: evolution and change. *CA Cancer J Clin* 2006;56:282-91.
2. Osuna D, De Alava E. Molecular pathology of sarcomas. *Rev Recent Clin Trials* 2009;4: 12-26.
3. Chou AJ, Geller DS, Gorlick R. Therapy for osteosarcoma: where do we go from here? *Pediatr Drugs* 2008;10: 315-27.
4. Thornton K. Chemotherapeutic management of soft tissue sarcoma. *Surg Clin North Am* 2008;88: 647-60.
5. Taylor BS, Barretina J, Maki RG, Antonescu CR, Singer S, Ladanyi M. Advances in sarcoma genomics and new therapeutic targets. *Nat Rev Cancer* 2011;11:541–57.
6. Nielsen TO, West RB. Translating gene expression into clinical care: sarcomas as a paradigm. *J Clin Oncol* 2010;28:1796–805.
7. Bovee JVMG, Hogendoorn PCW. Molecular pathology of sarcomas: concepts and clinical implications. *Virchows Arch* 2010;456:193–9.
8. Ye Y, Pringle LM, Lau AW, Riquelme DN, Wang H, Jiang T, et al. TRE17/USP6 oncogene translocated in aneurysmal bone cyst induces matrix metalloproteinase production via activation of NFkB. *Oncogene* 2010;29:3619–29.
9. Nielsen TO, West RB. Translating gene expression into clinical care: sarcomas as a paradigm. *J Clin Oncol* 2011; 28: 1796-805.
10. Wolden SL, Alektiar KM. Sarcomas across the age spectrum. *Semin Radiat Biol* 2010;20:45–51.
11. Verweij J. Soft tissue sarcoma trials: one size no longer fits all. *J Clin Oncol* 2009;27: 3085-87.
12. Demetri GD, von Mehren M, Antonescu CR, De Matteo RP, Ganjoo KN, Maki RG, *et al.* NCCN Task Force report: update on the management of patients with gastrointestinal stromal tumors. *J Natl Compr Cancer Netw* 2010;8 (Suppl 2): S1-41.
13. Shern JF, Chen L, Chmielecki J, Wei JS, Patidar R, Rosenberg M, Ambrogio L, Auclair D, Wang J, Song YK, et al. Comprehensive genomic analysis reveals a landscape of alterations affecting a common genetic axis in fusion-positive and fusion-negative tumors. *Cancer Discovery* 2014; 4: 216-31.

14. Stacchiotti S, Pantaleo MA, Negri T, Astolfi A, Conca E, Dagrada G, et al. Metastatic dermatofibrosarcoma protuberans (DFSP) and fibrosarcomatous DFSP (FS-DFSP): sensitivity to imatinib (IM) and gene expression profile. *J Clin Oncol* 2015; 33 suppl: Abstr 10553.
15. Georger B, Schulte J, Zwaan CM, Casanova M, Fischer M, Moreno L, et al. Phase I study of ceritinib in pediatric patients (Pts) with malignancies harboring a genetic alteration in ALK (ALK+): safety, pharmacokinetic (PK), and efficacy results. *J Clin Oncol* 2015; 33 suppl: Abstr 10005.
16. Park H, Garrido-Laguna I, Naing A, Fu S, Falchook GS, Piha-Paul SA, et al. Phase I study of the mTOR inhibitor sirolimus and the HDAC inhibitor vorinostat in patients with advanced malignancies. *J Clin Oncol* 2015; 33 suppl: Abstr 2584.
17. Kummar S, Allen D, Monks A, Polley EC, Hose CD, Ivy SP, et al. Cediranib for metastatic alveolar soft part sarcoma. *J Clin Oncol* 2013; 31: 2296-302.
18. Versleijen-Jonkers YM, Vlenterie M, van de Luijngaarden AC, van der Graaf WR. Anti-angiogenic therapy, a new player in the field of sarcoma treatment. *Crit Rev Oncol Hematol* 2014; 91: 172-85.
19. Ranieri G, Mammi M, Donato Di Paola E, Russo E, Gallelli L, Citraro R, et al. Pazopanib a tyrosine kinase inhibitor with strong anti-angiogenetic activity: a new treatment for metastatic soft tissue sarcoma. *Crit Rev Oncol Hematol* 2014; 89: 322-9.
20. Vistica DT, Hollingshead M, Borgel SD, Kenney S, Stockwin LH, Raffeld M, et al. Therapeutic vulnerability of an *in vivo* model of alveolar soft part sarcoma (ASPS) to antiangiogenic therapy. *J Pediatr Hematol Oncol* 2009;31: 561-70.
21. H. Bengtsson, K. Simpson, J. Bullard, Hansen K. aroma.affymetrix: A generic framework in R for analyzing small to very large Affymetrix data sets in bounded memory, Tech Report #745, Department of Statistics, University of California, Berkeley, February 2008 <http://statistics.berkeley.edu/tech-reports/745>.
22. Klooster R, Straasheijm K, Shah B, Sowden J, Frants R, Thornton C, et al. Comprehensive expression analysis of FSHD candidate genes at the mRNA and protein level. *Europ J Human Genet* 2009; 17: 1615-24.
23. Barretina J, Caponigro G, Stransky N, Venkatesan K, Margolin AA, Kim S, et al. The cancer cell line encyclopedia enables predictive modeling of anticancer drug sensitivity. *Nature* 2012; 483: 603-7.
24. Teicher BA. Searching for molecular targets in sarcoma. *Biochem Pharmacol* 2012; 84: 1-10.

25. Kollareddy M, Zheleva D, Dzubak P, Brahmshatriya PS, Lepsik M, Hajduch M. Aurora kinase inhibitors: progress towards the clinic. *Invest New Drugs* 2012; 30: 2411-32.
26. Teicher BA. Newer cytotoxic agents: attacking cancer broadly. *Clin Cancer Res* 2008; 14: 1610-6.
27. Mehra R, Serebriiskii IG, Burtneess B, Astsaturov I, Golemis EA. Aurora kinases in head and neck cancer. *Lancet Oncol* 2013; 14: e425-35.
28. Winter GE, Rix U, Lissat A, Stukalov A, Mullner MK, Bennett KL, et al. An integrated chemical biology approach identifies specific vulnerability of Ewing's sarcoma to combined inhibition of aurora kinases A and B. *Mol Cancer Ther* 2011; 10: 1846-56.
29. Maris JM, Morton CL, Gorlick R, Kolb EA, Lock R, Carol H, et al. Initial testing of the aurora kinase A inhibitor MLN8237 by the pediatric preclinical testing program (PPTP). *Pediatr Blood Cancer* 2010; 55: 26-34.
30. Carol H, Boehm I, Reynolds CP, Kang MH, Maris JM, Morton CL, et al. Efficacy and pharmacokinetic/pharmacodynamic evaluation of the aurora kinase A inhibitor MLN8237 against preclinical models of pediatric cancer. *Cancer Chemother Pharmacol* 2011; 68: 1291-304.
31. Gombos A, Metzger-Filho O, Dal Lago L, Awada-Hussein A. Clinical development of insulin-like growth factor receptor-1 (IGF-1R) inhibitors: at the crossroad? *Invest New Drugs* 2012; 30: 2433-42.
32. Chakraborty C, Doss CGP, Bandyopadhyay S. miRNAs in insulin resistance and diabetes-associated pancreatic cancer: the 'minute and miracle' molecule moving as a monitor in the 'genomic galaxy'. *Curr Drug Targets* 2013; 14: 1110-7.
33. Jackstadt R, Hermeking H. MicroRNAs as regulators and mediators of c-Myc function. *Biochim Biophys Acta* 2015; 1849: 544-53.
34. Sun C, Li N, Yang Z, Zhou B, He Y, Weng D, et al. miR-9 regulation of BRCA1 and ovarian cancer sensitivity to cisplatin and PARP inhibition. *J Natl Cancer Inst* 2013; 105: 1750-8.
35. Xu LF, Wu ZP, Chen Y, Zhu QS, Hamidi S, Navab R. MicroRNA-21 (miR-21) regulates cellular proliferation, invasion, migration and apoptosis by targeting PTEN, RECK and Bcl-2 in lung squamous carcinoma. *Plos One* 2014; 9: e103698.
36. Yang CH, Yue J, Pfeffer SR, Fan M, Paulus E, Hosni-Ahmed A, et al. MicroRNA-21 promotes glioblastoma tumorigenesis by downregulating IGFBP3. *J Biol Chem* 2014; 289: 25079-87.
37. Gadducci A, Sergiampietri C, Lanfredini N, Guiggi I. Micro-RNAs and ovarian cancer: the state of art and perspectives of clinical research. *Gynecol Endocrinol* 2014; 30: 266-71.

38. Li XJ, Luo XQ, Han BW, Duan FT, Wei PP, Chen YQ. MicroRNA-100/99a, deregulated in acute lymphoblastic leukemia, suppress proliferation and promote apoptosis by regulating the FKBP51 and IGF1R/mTOR signaling pathways. *Brit J Cancer* 2013; 109: 2189-98.
39. Britten CD. PI3K and MEK inhibitor combinations: examining the evidence in selected tumor types. *Cancer Chemother Pharmacol* 2013; 71: 1395-409.
40. Kolb EA, Gorlick R, Houghton PJ, Morton CL, Neale G, Keir ST, et al. Initial testing (Stage 1) of AZD6244 (ARRY-142886) by the Pediatric Preclinical Testing Program. *Pediatr Blood Cancer* 2010; 55: 668-77.
41. Wan X, Helman LJ. The biology behind mTOR inhibition in sarcoma. *The Oncologist* 2007; 12: 1007-18.
42. Carol H, Morton CL, Gorlick R, Kolb EA, Keir ST, Reynolds CP, et al. Initial testing (stage 1) of the Akt inhibitor GSK690693 by the pediatric preclinical testing program. *Pediatr Blood Cancer* 2010; 55: 1329-37.
43. Gorlick R, Maris JM, Houghton PJ, Lock R, Carol H, Kurashva RT, et al. Testing of the Akt/PKB inhibitor MK-2206 by the pediatric preclinical testing program. *Pediatr Blood Cancer* 2012; 59: 518-24.
44. Houghton PJ, Gorlick R, Kolb EA, Lock R, Carol H, Morton CL, et al. Initial testing (stage 1) of the mTOR kinase inhibitor AZD8055 by the pediatric preclinical testing program. *Pediatr Blood Cancer* 2012; 58: 191-9.
45. Kang MH, Reynolds CP, Maris JM, Gorlick R, Kolb EA, Lock R, et al. Initial testing (stage 1) of the investigational mTOR kinase inhibitor MLN0128 by the pediatric preclinical testing program. *Pediatr Blood Cancer* 2014; 61: 1486-9.
46. Filippakopoulos P, Knapp S. Targeting bromodomains: epigenetic readers of lysine acetylation. *Nature Rev Drug Discov* 2014; 13: 337-56.
47. Trabucco SE, Gerstein RM, Evens AM, Bradner JE, Shultz LD, Greiner DL, Zhang H. Inhibition of bromodomain proteins for the treatment of human diffuse large B-cell lymphoma. *Clin Cancer Res* 2015; 21: 113-22.
48. Dauphinot L, De Oliveira C, Melot T, Sevenet N, Thomas V, Weissman BE, Delattre O. Analysis of the expression of cell cycle regulators in Ewing cell lines: EWS-FLI-1 modulates p57KIP2 and c-Myc expression. *Oncogene* 2001; 20: 3258-65.
49. Toffolatti L, Frascella E, Ninfo V, Gambini C, Fomi M, Carli M, Rosolen A. MYCN expression in human rhabdomyosarcoma cell lines and tumor samples. *J Pathol* 2002; 196: 450-8.
50. Bouwman P, Jonkers J. Molecular pathways: how can BRCA-mutated tumors become resistant to PARP inhibitors? *Clin Cancer Res* 2013; 20: 540-7.

51. Murai J, Huang SYN, Renaud A, Zhang Y, Ji J, Takeda S, Morris J, Teicher B, Doroshow JH, Pommier Y. Stereospecific PARP trapping by BMN 673 and comparison with olaparib and rucaparib. *Mol Cancer Ther* 2013; 13: 433-43.
52. Garnett MJ, Edelman EJ, Heidorn SJ, Greenman CD, Dastur A, Lau KW, et al. Systematic identification of genomic markers of drug sensitivity in cancer cells. *Nature* 2012; 483: 570-5.
53. Brenner JC, Feng FY, Han S, Patel S, Goyal SV, Bou-Maroun LM, et al. PARP-1 inhibition as a targeted strategy to treat Ewing's sarcoma. *Cancer Res* 2012;72:1608–13.
54. Choy E, Butrynski JE, Harmon DC, Morgan JA, George S, Wagner AJ, et al. Phase II study of olaparib in patients with refractory Ewing sarcoma following failure of standard chemotherapy. *BMC Cancer* 2014; 14: 813.
55. Smith MA, Hampton OA, Reynolds CP, Kang MH, Maris JM, Gorlick R, et al. Initial testing of the PARP inhibitor BMN673 by the pediatric preclinical testing program: PALB2 mutation predicts exceptional in vivo response to BMN 673. *Pediatr Blood Cancer* 2015; 62: 91-8.
56. Fam HK, Walton C, Mitra SA, Chowdhury M, Osborne N, Choi K, et al. TDP1 and PARP1 deficiency are cytotoxic to rhabdomyosarcoma cells. *Mol Cancer Res* 2013; 11: 1179-92.
57. Guled M, Pazzaglia L, Borzel I, Mosakhani N, Novello C, Benassi MS, Knuutila S. Differentiating soft tissue leiomyosarcoma and undifferentiated pleomorphic sarcoma: a miRNA analysis. *Genes Chrom Cancer* 2014; 53: 693-702.
58. Kong LM, Liao CG, Zhang Y, Xu J, Li Y, Huang W, et al. A regulatory loop involving miR-22, Sp1, and c-Myc modulates CD147 expression in breast cancer invasion and metastasis. *Cancer Res* 2014; 74: 3764-78.
59. Kao CJ, Martinez A, Shi XB, Yang J, Evans CP, Dobi A, et al. MiR-30, as a tumor suppressor connects EGF/Src signal to ERG and EMT. *Oncogene* 2014; 33: 2495-503.
60. Mraz M, Chen L, Rassenti LZ, Ghia EM, Li H, Jepsen K, et al. MiR-150 influences B-cell receptor signaling in chronic lymphocytic leukemia by regulating expression of GAB1 and FOXP1. *Blood* 2014; 124: 84-95.
61. Fulda S. Molecular pathways: targeting inhibitor of apoptosis proteins in cancer- from mechanism to therapeutic application. *Clin Cancer Res* 2014; 20: 289-95.
62. Condon SM, Mitsuuchi Y, Deng Y, LaPorte MG, Rippin SR, Haimowitz T, et al. Birinapant, a smac-mimetic with improved tolerability for the treatment of solid tumors and hematological malignancies. *J Med Chem* 2014; 57: 3666-77.
63. Gong M, Ma J, Li M, Zhou M, Hock JM, Yu X. MicroRNA-204 critically regulates carcinogenesis in malignant peripheral nerve sheath tumors. *Neuro-Oncol* 2012; 14: 1007-17.

64. Avellino R, Carrella S, Pirozzi M, Risolino M, Salierno FG, Franco P, Stoppelli P, Verde P, Banfi S, Conte I. miR-204 targeting of Ankrd13A controls both mesenchymal neural crest and lens cell migration. *Plos One* 2013; 8: e61099.
65. Morrow CJ, Ghattas M, Smith C, Bonisch H, Bryce RA, Hickinson DM, Green TP, Dive C. Src family kinase inhibitor saracatinib (AZD0530) impairs oxaliplatin uptake in colorectal cancer cells and blocks organic cation transporters. *Cancer Res* 2010; 70: 5931-41.
66. Sakuma Y, Yamazaki Y, Nakamura Y, Yoshihara M, Matsukuma S, Nakayama H, et al. WZ4002, a third-generation EGFR inhibitor, can overcome anoikis resistance in EGFR-mutant lung adenocarcinomas more efficiently than Src inhibitors. *Lab Invest* 2012; 92: 371-83.
67. Ou DL, Shen YC, Yu SL, Chen KF, Yeh PY, Fan HH, et al. Induction of DNA damage-inducible gene GADD45 β contributes to sorfanib-induced apoptosis in hepatocellular carcinoma cells *Cancer Res* 2010; 70: 9309-18.
68. Shor AC, Keschman EA, Lee FY, Muro-Cacho C, Letson GD, Trent JC, et al. Dasatinib inhibits migration and invasion in diverse human sarcoma cell lines and induces apoptosis in bone sarcoma cells dependent on src kinase for survival. *Cancer Res* 2007; 67: 2800-8.
69. Dmitriev P, Petrov A, Anseau E, Stankevicius L, Charron S, Kim E, et al. The Kruppel-like factor 15 as a molecular link between myogenic factors and a chromosome 4q transcriptional enhance implicated in facioscapulohumeral dystrophy. *J Biol Chem* 2011; 286: 44620-31.

FIGURE LEGENDS

Figure 1. Constellation relational map showing response similarity connections among the approved and investigational anticancer agents tested in the sarcoma lines at a stringency of 0.75. The line thickness is directly proportional to the pair-wise correlation.

Figure 2. A. Chemical structures of eight aurora kinase inhibitors tested in the sarcoma lines. **B.** Heat map showing the IC_{50} response of the sarcoma lines, arranged by disease panel, for eight aurora kinase inhibitors. Green indicates $IC_{50} \geq 10^{-5}$; yellow indicates $IC_{50} \geq 10^{-7}$; red indicates $IC_{50} \geq 10^{-9}$; the blue box highlights the response of the Ewing sarcoma lines to the compounds. **C.** Concentration response curves for the 63 sarcoma lines and the Ewing sarcoma line panel to three aurora kinase inhibitors.

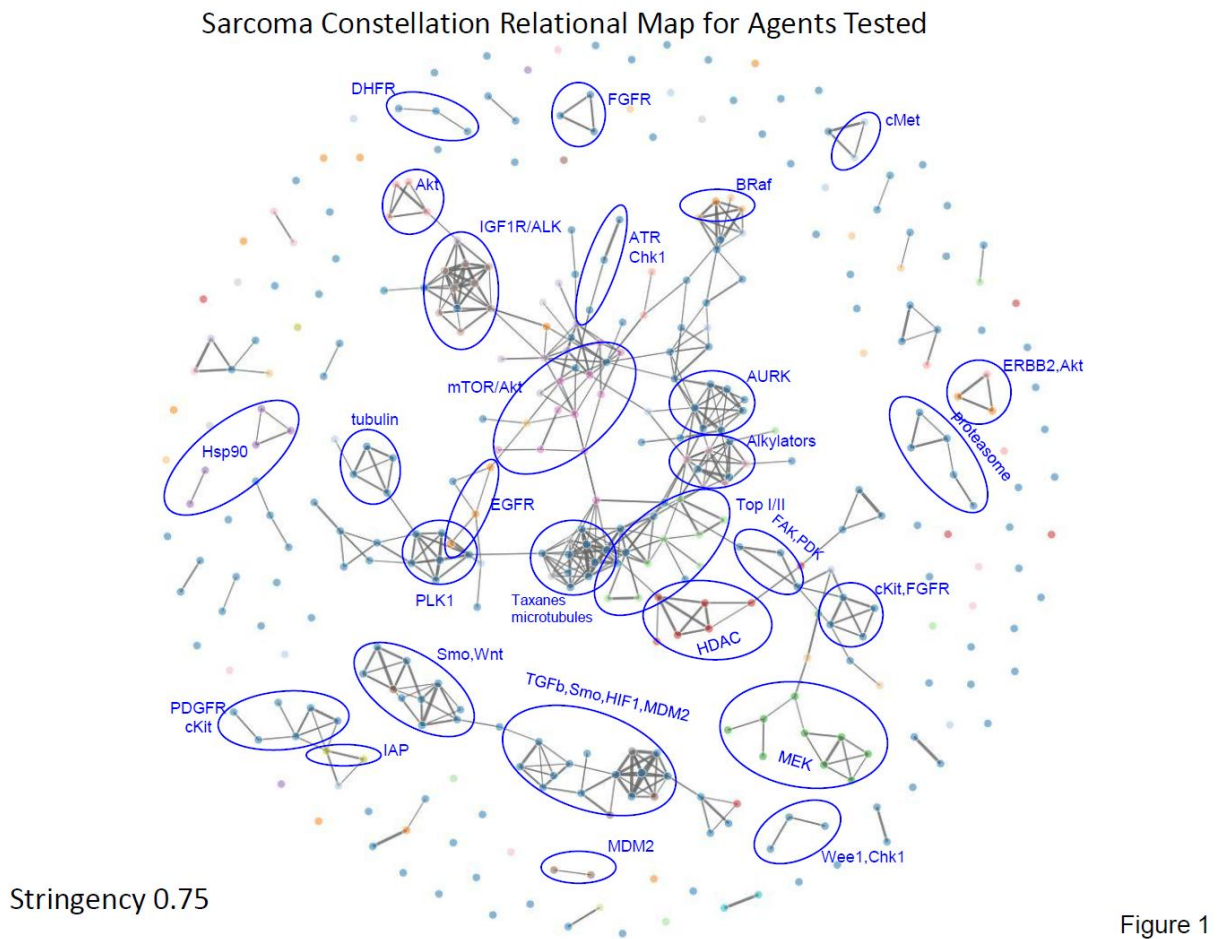
Figure 3. A. Chemical structures of eight insulin-like growth factor-1 receptor kinase inhibitors tested in the sarcoma lines. **B.** Heat map showing the IC_{50} response of the sarcoma lines, arranged by disease panel, for eight insulin-like growth factor-1 receptor kinase inhibitors. Green indicates $IC_{50} \geq 10^{-5}$; yellow indicates $IC_{50} \geq 10^{-7}$; red indicates $IC_{50} \geq 10^{-9}$; the blue box highlights the response of the rhabdomyosarcoma lines to the compounds. **C.** Concentration response curves for the 63 sarcoma lines and the rhabdomyosarcoma line panel to three insulin-like growth factor-1 receptor kinase inhibitors. **D.** Heat map of the sarcoma lines sorted by IC_{50} value for linsitinib along with \log_2 gene expression for ALK kinase, IGF2, IGF1 and IGF1R and microRNA expression from counts for miR-9-5p, miR-100-5p, miR-222-3p, miR-125-5p miR-22-3p and miR-21-5p. Red indicates low IC_{50} (high sensitivity) and low expression and green indicates high IC_{50} (resistance) and high expression.

Figure 4. A. Chemical structures of eight MEK kinase inhibitors tested in the sarcoma lines. **B.** Heat map showing the IC₅₀ response of the sarcoma lines, arranged by disease panel, for eight MEK kinase inhibitors. Green indicates IC₅₀ $\geq 10^{-5}$; yellow indicates IC₅₀ $\geq 10^{-7}$; red indicates IC₅₀ $\geq 10^{-9}$; black indicates not tested. **C.** Concentration response curves for the 63 sarcoma lines and the fibrosarcoma and leiomyosarcoma line panels to two MEK kinase inhibitors.

Figure 5. A. Chemical structures of the BET bromodomain inhibitors, JQ-1 and GSK-1210151A (I-BET-151). **B.** Heat map showing the IC₅₀ response of the sarcoma lines, arranged by disease panel, for two BET bromodomain inhibitors. Green indicates IC₅₀ $\geq 10^{-5}$; yellow indicates IC₅₀ $\geq 10^{-7}$; red indicates IC₅₀ $\geq 10^{-9}$; black indicates not tested. **C.** Heat map showing the log₂ gene expression of MYC (c-Myc), MYCN, and RUNX2 of the sarcoma lines, arranged by disease panel. Green indicates relatively high expression; yellow indicates mean expression; red indicates relatively low expression. The expression values are: MYC mean 8.55 (10.02-5.68); MYCN (Affymetrix cluster ID 2470838) mean 6.68 (10.62-5.42); MYCN (Affymetrix cluster ID 2470805) mean 7.8 (8.9-7.13) and RUNX2 mean 7.95 (11.18-5.55). **D.** Concentration response curves for the 63 sarcoma lines and the rhabdomyosarcoma, synovial sarcoma, Ewing sarcoma and osteosarcoma line panels to the BET bromodomain inhibitor JQ1.

Figure 6. A. Chemical structure of the PARP1 inhibitor talazoparib (BMN673). **B.** Heat map showing the log₂ gene expression of BRCA1, BRCA2, H2AFX, PARP1 and RAD51 of the sarcoma lines, arranged by disease panel. Green indicates relatively high expression; yellow indicates mean expression; red indicates relatively low expression. The expression values are: BRCA1 mean 6.92 (8.34-5.02); BRCA2 mean 6.37 (8.06-4.5); H2AFX mean 8.85 (9.88-7.74) PARP1 mean 9.23 (10.41-7.23) RAD51 mean 6.88 (8.58-4.71). Heat map showing the IC₅₀

response of the sarcoma lines, arranged by disease panel, for five PARP1 inhibitors. Green indicates $IC_{50} \geq 10^{-5}$; yellow indicates $IC_{50} \geq 10^{-7}$; red indicates $IC_{50} \geq 10^{-9}$; black indicates not tested. **C.** Concentration response curves for the 63 sarcoma lines and the Ewing sarcoma, malignant peripheral neural sheath tumors (MPNS), and synovial sarcoma line panels to the PARP1 inhibitor talazoparib. **D.** Heat map of the sarcoma lines sorted by IC_{50} value for talazoparib along with \log_2 gene expression for PARP1, BRCA2, BRCA1 and PLK2 and microRNA expression from counts for miR-100-5p, miR-222-3p, miR-574-3p miR-22-3p, miR-21-5p miR30a-5p, miR-150-5p and miR-9-5p. Red indicates low IC_{50} (high sensitivity) and low expression and green indicates high IC_{50} (resistance) and high expression.



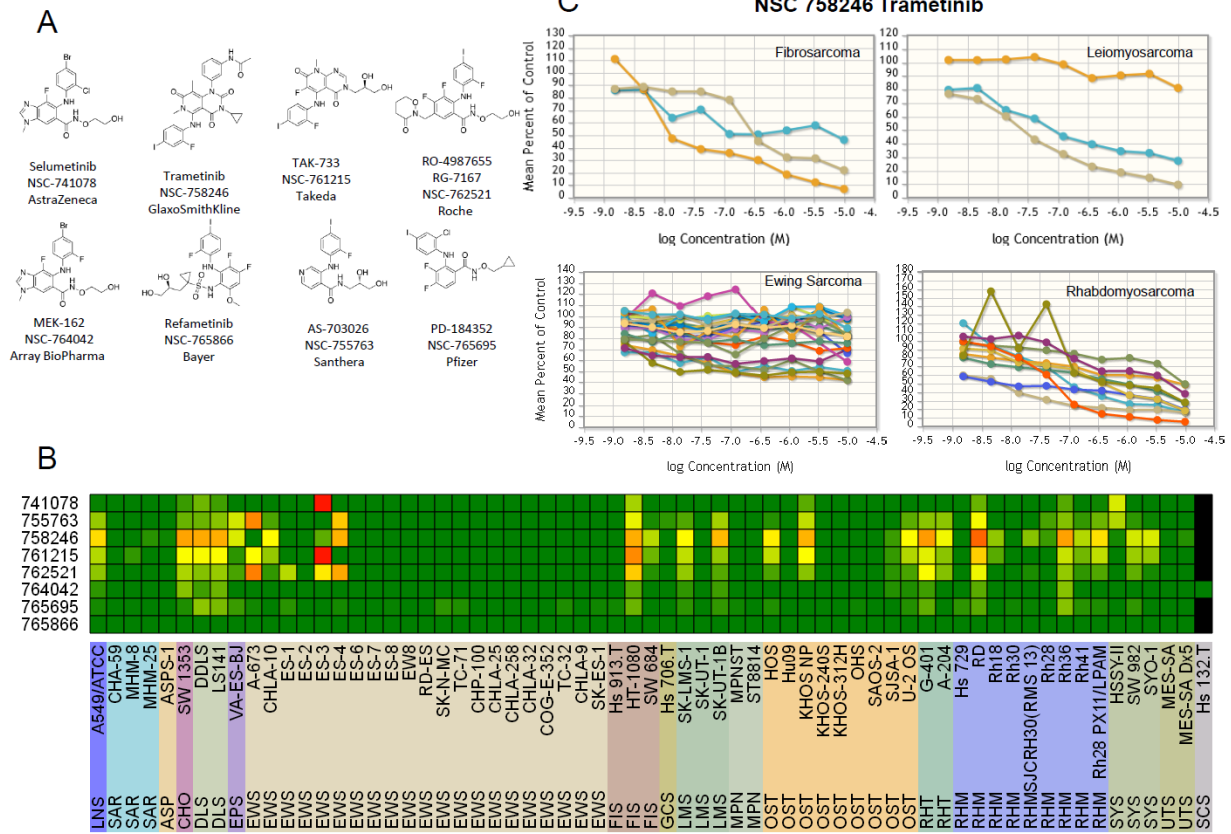


Figure 4

